Published in: ISIJ International, 38 (1998) 744-751

Austenite Grain Growth Behaviour of Microalloyed Al-V-N and Al-V-Ti-N steels

N. Gao and T. N. Baker
Metallurgy and Engineering Materials Group
Department of Mechanical Engineering
University of Strathclyde
Glasgow, Scotland, UK

Abstract

The austenite grain growth behaviour of microalloyed Al-V-N and Al-V-Ti-N steels has been studied. Estimations of austenite grain size for Al-V-N steels by several different grain growth inhibition models demonstrated that the best match to experimental results can be obtained from Gladman and Rios equations and it is AlN that controls the austenite grain size. The experimental and calculated results indicated that the drag force of plate-shaped AlN particles probably depends on their orientation and austenitising temperature. A modified Gladman model, which considers the effects of complex arrays of different types of particles on the stabilized austenite grain size, can be used to predict the austenite grain size and particle size for an Al-V-Ti-N steel when the combined effect of AlN and TiN is considered.

KEY WORDS: carbonitride; microalloyed steel; austenite grain growth.

1. Introduction

High-strength low-alloy structural (HSLA) steels are very important metallic materials. Their outstanding properties are high strength, resistance to brittle fracture, cold formability, and good weldability. They now have various applications including line-pipe, off-shore structures and the automotive industry. Grains in HSLA steels may coarsen either by normal primary grain coarsening or abnormal grain coarsening. The characteristic features of normal grain growth can be seen in steels without grain refining particles which show a gradual increase in grain size with increasing temperature.[1–2] In the presence of pinning particles however, the grain growth process frequently occurs by the growth of a few selected grains to abnormally large dimensions and other grains will not be able to grow until further particle coarsening has occurred. This type of grain growth is known as abnormal grain growth or secondary recrystallization.[3–4] Abnormal grain growth can only occur when normal grain growth is inhibited and is particularly likely to occur as the temperature is raised and as the particle dispersion becomes unstable.[5] The abnormal grain growth might occur due to the presence of additional heterogeneities, e.g. in the particle distribution. Where locally, the ratio of the particle size r to the volume fraction f is larger than the mean value r/f, some grains might start to grow preferentially. This situation of abnormal grain growth is accompanied by an increase in the heterogeneity parameter Z defined as the ratio of the size of a growing grain to the size of the neighbouring grains.[6–7]

Although there have been some studies of the effect of carbides and nitrides on the austenite grain coarsening temperature, however, there are still a number of questions

pertaining to both the function of Al and Ti in vanadium microalloyed steels and their influence on austenite grain growth, which should be investigated further in order to understand the relative importance of the interaction of V with Al and Ti in microalloyed steels. In addition, the subject of the evaluation of these process is still of interest.

2. Experimental Procedure

The steels used in the study are four commercial high strength Al-V-N steels and one Al-V-Ti-N steel whose compositions are given in Table 1. The specimens were austenitised for 0.5 hour in an argon atmosphere at temperatures between $900^{\circ}C$ and $1200^{\circ}C$ and water quenched, followed by tempering at $650^{\circ}C$ for 2 hours and air cooling to room temperature. A Chromel-Alumel thermocouple connected to a digital millivoltmeter was bound on the specimens and recorded the temperature**.**

Table 1. Compositions of Experimental Steels, wt%

No.	C	Si	Mn	P	S	Al	N	V	Ti
1	0.13	0.30	1.43	0.010	0.003	0.032	0.002	0.10	-
2	0.12	0.31	1.43	0.011	0.002	0.037	0.015	0.10	-
3	0.12	0.31	1.45	0.011	0.003	0.026	0.0049	0.10	-
4	0.13	0.30	1.45	0.012	0.003	0.029	0.0043	0.049	-
Ti Steel	0.074	0.37	1.53	0.013	0.007	0.027	0.018	0.13	0.012

Metallographic specimens were prepared by conventional techniques and austenite grain boundaries were revealed by etching in 4 g picric acid, 100 ml methanol plus a few drops teepol at 80-$90^{\circ}C$ for 2-3 min. A linear intercept method was employed to assess the austenite grain size. About 300 to 400 intercepts were counted for each specimen. Extraction replicas were obtained by evaporating carbon on to the etched specimens in a

Mikro BA3 Balzers Vacuum Coating Unit at 5×10^{-5} torr. The examination for precipitate size, distribution and compositions was performed in a Philips EM 400T transmission electron microscope (TEM), operated at 100 KV, which was interfaced to an EDAX 9100 energy dispersive system. The size of particles were measured either directly on the screen at a suitable magnification or by measuring enlarged micrographs. At least 200 particles were measured for each specimen to give the mean particle size.

3. Experimental Results

3.1. Austenite Grain Growth Behaviour

The austenite grain coarsening behaviour as a function of temperature is shown in **Fig. 1**. Except for the Al-V-Ti-N steel, all other Al-V-N steels clearly show two-stage grain growth. Below a critical temperature range, defined as the grain coarsening temperatures, the change in grain size is very small, while above this critical temperature range the grain size increases with temperature very rapidly. In the grain coarsening temperature ranges there is a duplex structure represented by the cross-hatching in Fig. 1. This kind of abnormal grain growth in the grain coarsening temperature range is clearly shown in **Fig. 2(a).** When the temperatures were higher than the grain coarsening temperatures, the dissolution of precipitates in the steels allows more grains to grow, which is considered to be a normal process (see **Fig. 2(b)**). It should be noted that this kind of two-stage grain growth and mixed grain growth behaviour will not be reflected if only the average of the grain size measurement is given. As expected for the Ti free steels, Steel 2 with high Al and N contents possesses the highest grain coarsening temperature, which is about 1100-

1150°C. The grain coarsening temperatures for the three low Al and N steels are about 950-1000°C. Steel 1 with lowest volume fraction of AlN among these steels has the largest grain size at 950°C.

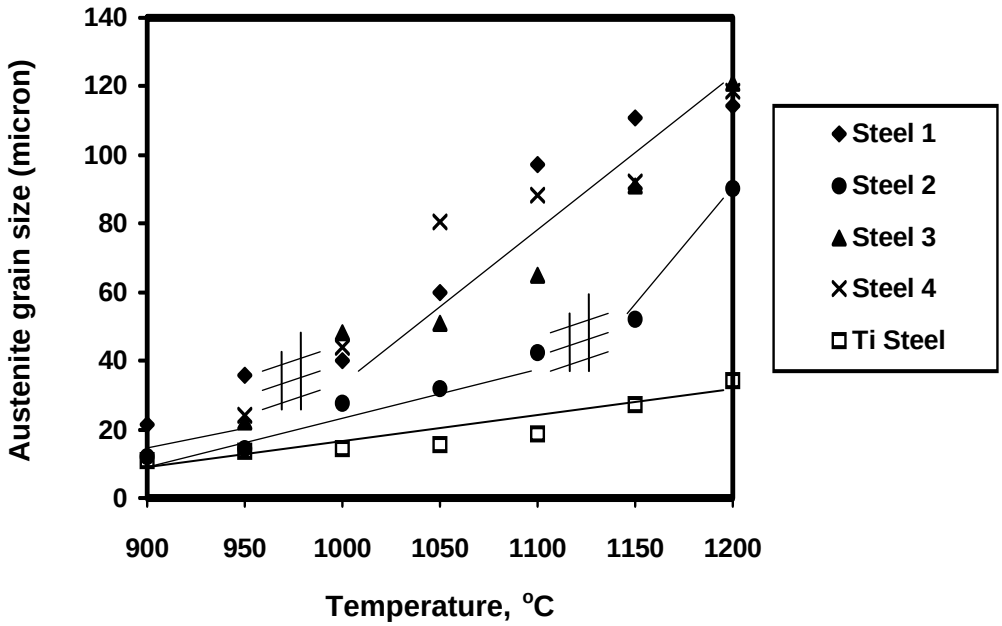

Fig. 1 Variation of prior austenite grain size with temperature for Al-V-N and Al-V-Ti-N steels.

From the bottom graph in Fig. 1, it can be seen that compared with the austenite grain size of the other four Al-V-N steels, the Al-V-Ti-N steel has the smallest austenite grain size. Another obvious feature is that in contrast with other Al-V-N steels which followed an abnormal grain growth behaviour, the austenite grain growth of the Al-V-Ti-N steel retains a steady slow growth up to 1200°C, i.e. it has the characteristics of normal grain growth.

3.2 Particle Sizes and Distributions

The size of VC particles in as-rolled steels were measured and their mean and the number of precipitates per unit area (μm^2) were calculated (see **Table 2)**. The average length and width of AlN particles in as-rolled steels were found to be 105 and 49 nm respectively. The size of AlN particles in Steel 2 were measured for each quenched specimen after solution treatment at 900, 1050 and 1150$^\circ C$. **Table 3** and **Fig. 3** record the particle size distributions in length, width and radius with the change in temperature. The radius of AlN particle was assumed to equal half of the average of the particle length and width. In general, the particle sizes decreased but the number of particles less than 30 nm in radius increased with increasing temperature. It is interesting to note that there are similar particle size distributions at 1050$^\circ C$ and at 1150$^\circ C$. The latter temperature corresponds to the grain coarsening temperature for Steel 2 (see Fig. 1). This may indicate that the process of particle coalescence and dissolution is occurring simultaneously in these temperature ranges**.**

Table 2. Distribution of VC Particle Size for As-rolled Steels

No.	Total area, μm^2	No. of particles	No. of particles per unit area, μm^{-2}	Mean particle size, nm
1	21.0	525	25	9.4
2	21.0	434	21	14.4
3	21.0	743	36	8.7
4	21.0	521	25	8.3

TEM observations with EDAX analyses have proved that there are many AlN and TiN particles in the Al-V-Ti-N steel, Steel 5. With temperature increasing from 900 to 1200$^\circ C$, the number of AlN particles decreased. Particles sizes in Steel 5 have also been measured from replicas using TEM for each specimen quenched from 950, 1100 and

1200°C. **Table 4** and **Fig. 4** demonstrate that the particle size increases slightly from 900 to 1100°C due to particle coarsening and then the particle size decreases from 1100 to 1200°C due to dissolution of particles. Because the particle sizes of AlN and TiN in this steel are in same range and their morphologies are quite similar, it was not intended to identify the particles when the particle average size and distribution were determined. Therefore, the data in Table 4 and Fig. 4 for Steel 5 are the results of contributions from both AlN and TiN particles.

Table 3 Distribution of AlN Particle Size at Different Austenitising Temperature for Steel 2

T, °C	Number of Particles	Average Length, nm	Average Width, nm	Average Radius, nm
900	228	98	55	38
1050	214	74	45	30
1150	208	76	45	31

Table 4 Distribution of Particle Size at Different Austenitising Temperature Al-V-Ti-N Steel

T, °C	Number of Particles	Average Length, nm	Average Width, nm	Average Radius, nm
950	225	47	38	21
1100	222	57	44	25
1200	220	34	32	17

4. Discussion

4.1. Abnormal Grain Growth

It is usual to distinguish between two kinds of grain growth: normal and abnormal. During normal grain growth, the grain size distribution evolves approximately uniformly, like that which occurs in C-Mn steels. When the microstructure becomes unstable a few grains may grow excessively, consuming the smaller recrystallized grains. This process,

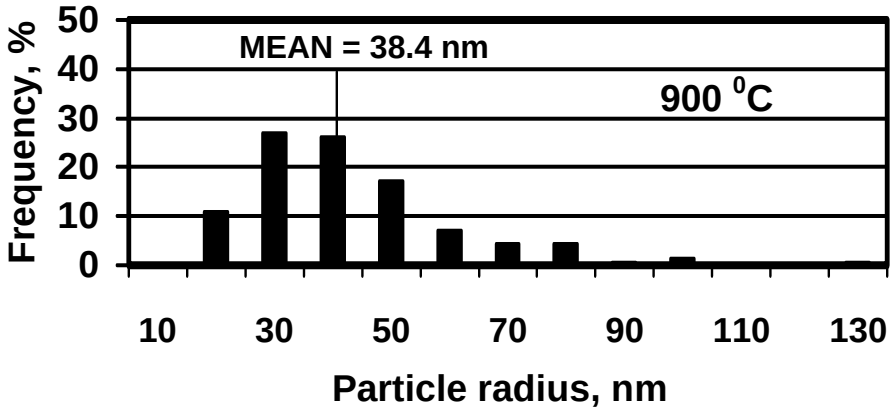

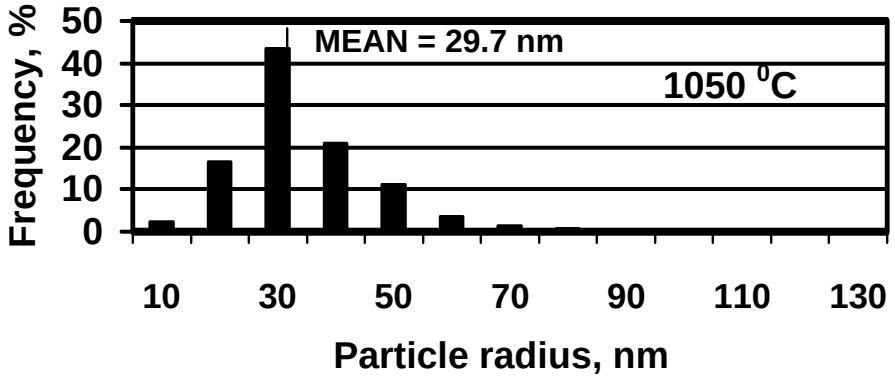

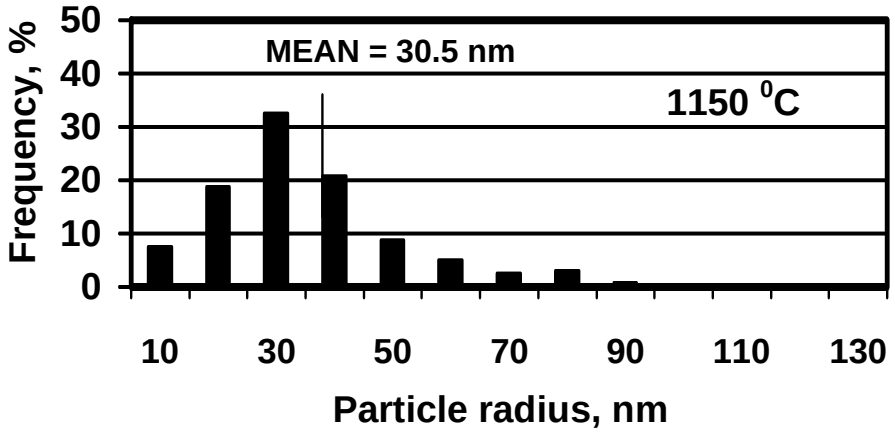

Fig. 3 Distribution of AlN particle radius at different quenching temperatures for Steel 2.

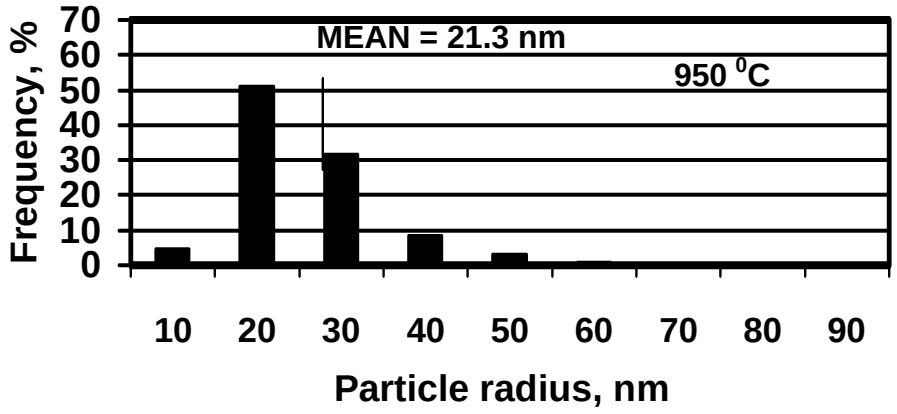

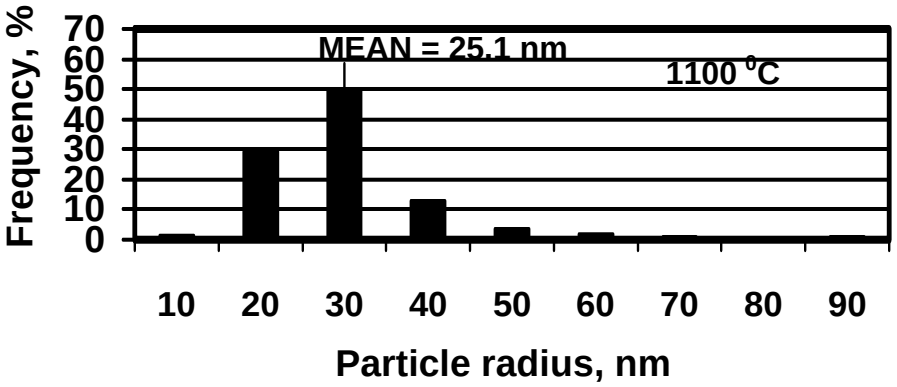

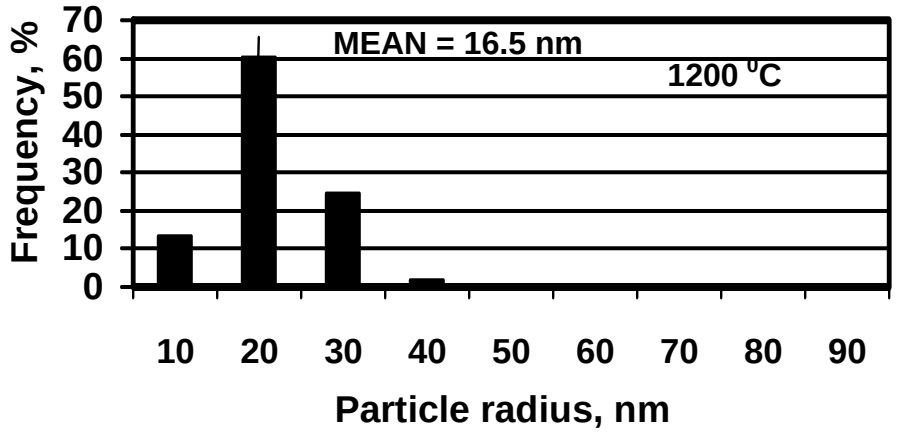

Fig. 4 Distribution of particle radius at different quenching temperatures for Ti Steel.

which may lead to grain diameters of several millimeters or greater, is known as abnormal grain growth or secondary recrystallization. The driving force for abnormal grain growth is usually the reduction in grain boundary energy as for normal grain growth. Abnormal grain growth can only occur when grain growth is inhibited. The main factors which lead to abnormal grain growth are second-phase particles, texture and surface effects.[5,8–9] The conditions for abnormal grain growth can be established in different ways[4] and under these conditions, only the few grains that have the largest size advantage would grow. The final secondary recrystallized grain size would be dictated by the frequency of occurrence of abnormal grain growth, since their collision would then terminate the growth process.

The characteristic features of abnormal grain growth were found in the current Al-V-N steels presented in Figs. 1 and 2(a). It can be seen that fine grains persist up to the grain coarsening temperature, followed by a mixed grain size due to abnormal grain growth. At temperatures much higher than the grain coarsening temperature, significant dissolution of the grain refining particles results in a grain growth process which is again regarded as normal growth. It has been observed that grain-coarsening occurs at temperatures below those required for complete dissolution of the precipitate particles in the steels.[3] This indicates that for a given volume fraction, growth of the particles to a size in excess of the critical particle radius, r_{crit}, will result in grain-coarsening.

A phenomenological relation between steel composition and grain coarsening temperature has been derived from the experimental data for similar Al, V steels.[10] Under the conditions of these experiments undertaken between 950 and 1250 $^{\circ}C$, there

appears to be a linear increase in the observed grain-coarsening temperature, T_c, with the temperature for complete solution of the microalloyed carbide or nitride, T_s, that is,

$$T_c = A + BT_s = A + B\left(\frac{Q}{P - \log(M \times C)} - 273\right), ^\circ C \qquad (1)$$

Here A and B are the intercept and slope of the line segments for the curves of observed grain-coarsening temperature and the temperature for complete solution of the microalloy carbide or nitride. Q and P are constants from published solubility data.[10] For AlN, A and B were given as 385 and 0.535 respectively. Taking the Al and N contents of the present four steels (wt%) with the above equation as M and C, the results of T_c are as 931, 1059, 967 and 966 $^\circ C$ respectively, in fairly close agreement with the measured grain-coarsening temperature range (See Fig. 1).

4.2. The Evaluation of Austenite Grain Size

It has been known for many years that particles can restrain the growth of austenite grains.[6,11–13] Several theoretical interpretations of grain growth in particle-containing materials have been put forward. The model developed by Zener[14] produces a simple relationship

$$R_Z = \frac{4r}{3f} \qquad (2)$$

between the grain radius R, the particle volume fraction f and particle radius r. He considered that both grains and particles could be approximated to spheres.

Gladman[6] adopted a more realistic approach by considering the pinning force exerted by a single particle on a planar boundary and then derived the driving force for grain

growth. An important feature in this model is the ratio of the radii of growing grains to matrix grains, Z .

$$R_G = \frac{\pi r}{6f}\left(\frac{3}{2} - \frac{2}{Z}\right) \tag{3}$$

where Z lies between $\sqrt{2}$ and 2.

Hellman and Hillert[15] considered the curvature in the grain boundary and introduced into Zener's equation a correction factor β which equalled to $0.125Ln(40R/r)$, and for abnormal grain growth the equation was derived as

$$R_{H_1} = \frac{4r}{3f\beta} \tag{4}$$

where β was normally between 1.3 to 1.6.

In recent years, computer modelling has been developed to predict particle-size / grain-size relationships. Hillert[16] compared these models with both two and three dimensional approaches discussed in the literature. He concludes that in three dimensional systems

$$R_c = \frac{4r}{9f^{0.93}} \tag{5}$$

is recommended, except for large values of f , where the exponent decreases to lower values.

Rios[17] derived an equation to predict grain growth in systems in which particles are coarsening and dissolving where

$$R_R = \frac{r}{6f} \tag{6}$$

Another model, developed by Elst *et al*,[7] can be modified to accommodate elongated particles, a bimodal particle distribution and a distribution of grain boundary precipitates. Here

$$R_E = \frac{4r}{3f\beta}\left(\frac{3}{2} - \frac{2}{Z}\right) \qquad (7)$$

where β is an increasing function of R/r and R_E approximated to 0.056~0.067$\left(r/f\right)$.[18]

In the present work an attempt has been made to compare the above equations with experimental data for r, in order to evaluate the austenite grain size for present Al-V-N as-rolled steels, as it was not found to be possible to measure this from metallographically prepared specimens. Calculations based on the stoichiometry indicate that there are two main kinds of particles in the steels, i.e. VC and AlN. Since AlN was precipitated at higher temperatures than VC, the two particle compositions were considered separately. Both the volume fractions f of AlN and VC, were calculated from the binary solubility data[19–20] and the composition of steels, assuming stoichiometry. The data of the particle size are taken from experimental results (see Table 2). It was found that when VC particles were considered, the values of the austenite grain size calculated by these equations are much smaller than expected values, and are in the range of 0.02-4.8 μm, even smaller than the measured ferrite grain sizes. However, when considering only AlN particles in the steels, the calculated austenite grain sizes fall into a reasonable range (**Table 5**). The influence of AlN on grain size was clearly demonstrated for Steel 2 which has high Al and N contents, and the smallest austenite grain size. This is consistent with the results measured for the ferrite grain sizes.[21] Among the four steels

examined, the smallest ferrite grain size occurred in Steel 2, which was inherited from the small austenite grain.

Table 5. Evaluations of Austenite Grain Size from Considration of AlN by Different Grain Growth Inhibition Models for As-Rolled Steels

No.	$f \times 10^3$	r/f	R_Z μm	R_G μm	R_{H_1} μm	R_{H_2} μm	R_R μm	R_E μm
1	0.143	273	364	72	251	65	46	18
2	1.073	36	48	9.4	33	10	6.0	2.4
3	0.351	111	148	29	102	28	19	7.4
4	0.307	127	169	33	117	32	21	8.5

Because the particle size data used for calculation in above equations was taken from as-rolled steels, which were continuously cooled from the high temperature austenite region to ferrite, it cannot be compared with the results from the austenite grain coarsening experiments, in which specimens were heated to temperatures high in the austenite region and then quenched in water. To evaluate accurately the austenite size for the as-rolled steels after rolling is impossible. However, the austenite grain size in as-rolled steels should be similar to the austenite grain size in the low temperature austenite region for the steels in austenite grain coarsening experiments (shown in Fig. 1). It is clear from Table 5, that the Zener equation overestimates the austenite grain size, as indicated in several papers.[3,17] The predicted values of the austenite grain size estimated by the Gladman and by the Rios equations are fairly close to the present austenite grain coarsening experimental results at $950^\circ C$ (see **Fig. 5**), while those from Hellman and Elst equations are not. Fig. 5 also includes the data from Tweed et al..[22] The results of the above calculations also indicated that for the present Al-V-N steels, it is AlN as expected, and not VC that controls the austenite grain size for the as-rolled steels.

Although there are larger volume fractions of VC with smaller particle sizes in the steels, most VC particles precipitate during cooling in ferrite after rolling which contributes to the dispersion strengthening but is too late to inhibit austenite grain growth. Therefore, from the point of view of controlling austenite grain growth, it is beneficial for vanadium microalloyed steels at the levels of V used in the present work to contain some Al.

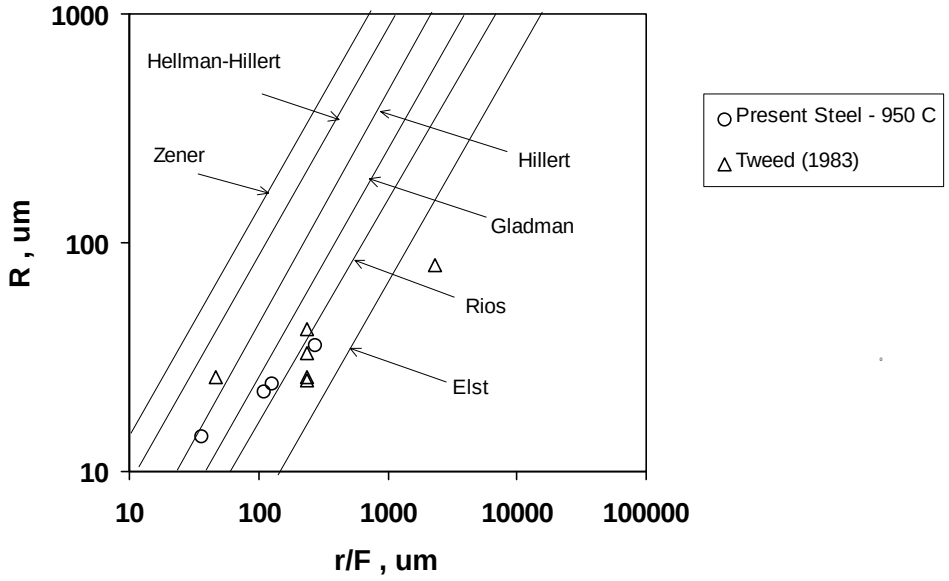

Fig. 5.3 Comparing experimental data with different grain growth inhibition models

4.3. The Evaluation of AlN Particle Size in Al-V-N Steels

In order to examine further the reliability of the different grain growth inhibition models, the AlN particle size was firstly calculated by the different equations for the present steels, austenitised and then quenched between $900^{\circ}C$ and $1200^{\circ}C$. A comparison was then made between the calculated results shown in **Table 6** and the

measured results given in Table 3. The austenite grain size , R, was taken from experimental data shown in Fig. 1, and the volume fraction of AlN, f_{AlN}, for the different austenitising temperatures was calculated from the following equations [21)]

$$(AlN) = \frac{(A_{Al} + A_N)}{2A_N}\left\{\left(N_0 + Al_0 \times \frac{A_N}{A_{Al}}\right) - \left[\left(N_0 + Al_0 \times \frac{A_N}{A_{Al}}\right)^2 - \frac{4A_N}{A_{Al}}\left(Al_0 \times N_0 - K_{AlN}\right)\right]^{1/2}\right\} \quad (8)$$

and $$K_{AlN} = \exp(-7750/T + 1.80) \quad (9)$$

$$f_{AlN} = \frac{(AlN) \times \rho_m}{100 \times \rho_{AlN}} \quad (10)$$

where Al_0 and N_0 are from the present the alloy composition, and A_{Al} and A_N the atomic masses of aluminium and nitrogen respectively. (AlN) is the amount of AlN precipitated from the matrix, while K_{AlN} is the solubility product of AlN. All are expressed as weight percent. $\rho_m = 7.8 kgm^{-3}$ is the density of the steel, and $\rho_{AlN} = 3.2 kgm^{-3}$ is the density of AlN.

Table 6. Evaluations of AlN Particle Size by Different Grain Growth Inhibition Models for Austenitised Steel 2

T, $^\circ C$	$f \times 10^3$	$R_{measured}$ μm	r_Z nm	r_G nm	r_{H_1} nm	r_{H_2} nm	r_R nm	r_E nm
900	0.968	12.2	8.9	45.1	12.9	43.2	71	176
950	0.905	14.2	9.6	49.1	14.0	47.2	77	192
1000	0.822	27.6	17.0	86.7	24.7	84.0	136	339
1050	0.716	31.8	17.1	87.0	24.8	85.1	137	340
1100	0.587	42.5	18.7	95.3	27.2	94.5	150	373
1150	0.433	52.0	16.9	86.0	24.6	87.2	135	336
1200	0.253	90.4	17.2	87.4	24.9	91.9	137	342

The volume fraction of AlN, f_{AlN}, decreases with increasing austenitising temperature for the four tested steels and obviously there is more AlN in Steel 2 with high Al and N contents than in the other steels. From Fig. 3 and Tables 3 and 6, it can be seen that with respect to the average radius of AlN particles, the Gladman (r_G) equation again provides the best match to the experimental data, especially in the low temperature austenite range. This is consistent with the results obtained for the as-rolled steels calculated above. However, an interesting result is that when the austenitising temperature increases to above $1000^\circ C$, the AlN size required to inhibit austenite grain growth tends to be closer to the average length of the AlN particle than the average radius.

It should be pointed out that all of the above grain growth inhibition models always assume the particle shape to be spherical. However, in high strength low alloy steels, it has been shown that the shape of the precipitate depends on composition.[23] Second phase particles are not usually spheres, but more often are needle- or plate-shaped, like the plate-shaped AlN in the current steels. The assumption that all the particles are spherical is thus not very realistic.[24] It may be argued that often second phase particles have a random orientation in the matrix and the mean drag force probably approximates to the drag from a spherical particle. There are, however, many cases where plate- or needle-shaped particles have a preferred orientation within the material. The geometric shape of the second phase particles strongly affects the magnitude of the drag force.[5,25–26] The interaction of a boundary with cubic particles has been analysed by Ringer et al..[27] It was demonstrated that the strength of the interaction depends upon the orientation of the cube relative to the boundary and in the extreme case, when the cubic side is parallel to the boundary, the drag force is almost twice that of a sphere of the same

volume. Therefore, the effect of the particle shape is a rather more important factor than the effect of the nature of the particle interface.[24)]

Concerning the effect of particle shape, for both our experimental and calculated results, it seems that for the present Al-V-N steels, the length of AlN particles plays a more important role at high temperature, as grain boundary diffusion and grain boundary motion are more easy. It is suggested that the average radius of AlN particles is responsible for controlling austenite grain growth in the low austenitising temperature range and the average length of AlN particle in the high austenitising temperature range. A typical example of AlN particles associated with grain boundaries from Steel 2 at $900^{\circ}C$ and $1050^{\circ}C$ is shown in **Fig. 6**.

4.4. The Evaluation of Particle Size in Al-V-Ti-N Steels

It is expected that a normal austenite grain growth behaviour will be followed in a Al-V-Ti-N steel because the AlN and TiN particles in the Al-V-Ti-N steel do not go completely into solution until above $1200^{\circ}C$,[28–29)] although AlN particles will gradually dissolve with increasing temperature below $1200^{\circ}C$.[30)] Calculations based on the stoichiometry of TiN, AlN and VN and steel composition, indicate that in this steel there is sufficient nitrogen to form TiN and AlN and almost no nitrogen left for VN. Therefore, only AlN and TiN particles are considered to play a role in inhibition of austenite grain growth for this steel.

Using the same method as for the other Al-V-N steels considered previously, six different grain growth inhibition models developed separately by Zener, Gladman, Hellman, Hiller, Rios and Elst were investigated to evaluate the particle size in the Al-V-

Ti-N steel. One difference is that for normal grain growth, Hellman and Hillert[15] proposed an alternative equation

$$R'_{H_1} = \frac{4r}{9f\beta} \tag{11}$$

A comparison was made between the calculated results respectively for AlN particle size shown in **Table 7,** for TiN particle size shown in **Table 8**, and the measured results given in Table 4. The austenite grain size , R, was taken from the experimental data shown in Fig. 1. The volume fraction of AlN, f_{AlN}, and the volume fraction of TiN, f_{TiN}, for the different austenitising temperatures were calculated from the following equations[21]

$$N_S = \frac{1}{2}\left(N_0 - Al_0 \times \frac{A_N}{A_{Al}} - Ti_0 \times \frac{A_N}{A_{Ti}} \right) + \frac{1}{2}\left[\left(N_0 - Al_0 \times \frac{A_N}{A_{Al}} - Ti_0 \times \frac{A_N}{A_{Ti}} \right)^2 + 4\left(K_{AlN} \times \frac{A_N}{A_{Al}} + K_{TiN} \times \frac{A_N}{A_{Ti}} \right) \right]^{1/2} \tag{12}$$

$$(AlN) = \left(Al_0 - \frac{K_{AlN}}{N_S} \right) \times \left(\frac{A_{Al} + A_N}{A_{Al}} \right) \tag{13}$$

$$(TiN) = \left(Ti_0 - \frac{K_{TiN}}{N_S} \right) \times \left(\frac{A_{Ti} + A_N}{A_{Ti}} \right) \tag{14}$$

and $$K_{AlN} = \exp(-7750/T + 1.80) \tag{15}$$

$$K_{TiN} = \exp(-15020/T + 3.82) \tag{16}$$

$$f_{AlN} = \frac{(AlN) \times \rho_m}{100 \times \rho_{AlN}} \tag{17}$$

$$f_{TiN} = \frac{(TiN) \times \rho_m}{100 \times \rho_{TiN}} \qquad (18)$$

where Ti_0 is for the present alloy composition and A_{Ti} the relative atomic mass of titanium. (TiN) is the weight of TiN precipitated from the matrix, while K_{TiN} is the solubility product of TiN. All are expressed as weight percent. $\rho_{TiN} = 5.4 g/cm^3$ is the density of TiN.

Table 7. Evaluations of AlN Particle Size by Different Grain Growth Inhibition Models for Austenitised Ti Steel

T, $^\circ C$	f_{AlN} $\times 10^3$	$R_{measured}$ μm	r_Z nm	r_G nm	r_{H_1} nm	r_{H_2} nm	r_R nm	r_E nm
900	0.813	10.7	6.5	33.2	25.5	32.2	52.2	130
950	0.739	13.5	7.5	38.1	29.2	37.2	59.9	149
1000	0.647	14.2	6.9	35.1	26.9	34.6	55.1	137
1050	0.537	15.7	6.3	32.2	24.7	32.1	50.6	126
1100	0.402	18.8	5.7	28.9	22.2	29.4	45.4	113
1150	0.244	27.3	4.6	23.4	17.9	26.8	36.7	91.4
1200	0.061	34.3	1.6	8.1	6.2	9.4	12.7	31.5

Table 8. Evaluations of TiN Particle Size by Different Grain Growth Inhibition Models for Austenitised Ti Steel

T, $^\circ C$	f_{TiN} $\times 10^3$	$R_{measured}$ μm	r_Z nm	r_G nm	r_{H_1} nm	r_{H_2} nm	r_R nm	r_E nm
900	0.2240	10.7	1.8	9.2	7.0	9.7	14.4	35.8
950	0.2240	13.5	2.3	11.5	8.9	12.3	18.1	45.1
1000	0.2240	14.2	2.4	12.2	9.3	12.9	19.1	47.5
1050	0.2240	15.7	2.6	13.5	10.3	14.3	21.1	52.6
1100	0.2239	18.8	3.2	16.1	12.3	17.1	25.3	62.9
1150	0.2237	27.3	4.6	23.3	17.9	24.8	36.4	91.2
1200	0.2235	34.3	5.8	29.3	22.5	31.1	46.0	114.5

Fig. 7 demonstrates that the volume fraction of AlN, f_{AlN}, decreases with increasing austenitising temperature, while the volume fraction of TiN, f_{TiN}, is almost constant at

all temperatures. From Tables 7 and 8, it was found that compared with the experimental data in Table 4, none of the six grain growth inhibition models can provide satisfactory results when an individual particle size, either as AlN or TiN, was evaluated independently by above models, although the Rios model seems to give close results at low austenitising temperatures but not at high temperatures.

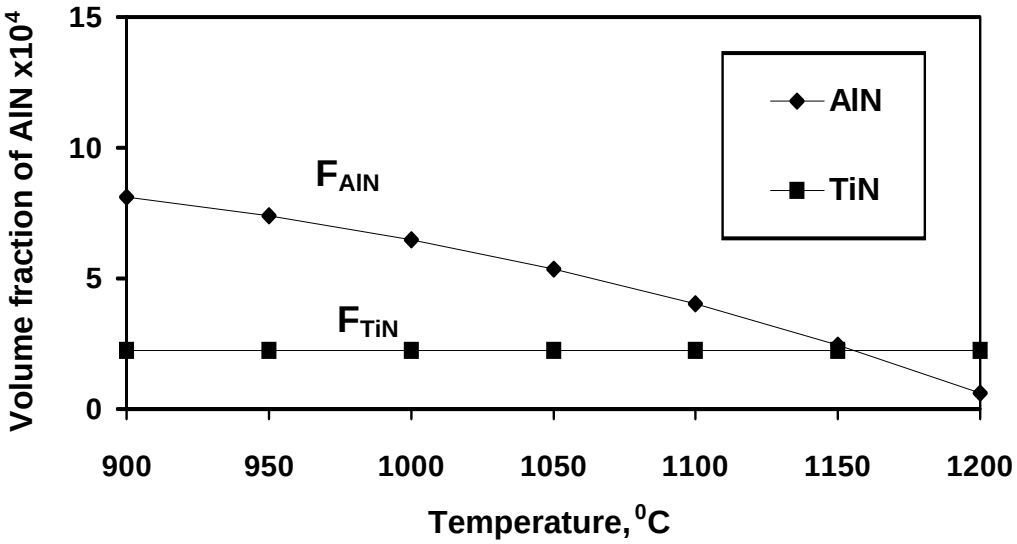

Fig. 7 The volume fraction of AlN and TiN as a function of temperature for Al-V-Ti-N Steel.

The effects of complex arrays of different types of particles on the stabilized austenite grain size have been considered by a new model developed recently by Gladman.[31–32] This model assumes that the grain growth can be inhibited by an array of different species of particle, each having a volume fraction f_i and a particle radius r_i

$$R_G^{'} = \frac{(1-4/3Z)}{\sum(f_i/r_i)} \qquad (19)$$

In the current Al-V-Ti-N steel, only AlN and TiN particles were considered, thus from equation (19), this gives

$$R_G^{'} = \frac{(1 - 4/3Z)}{\left(\frac{f_{AlN}}{r_{AlN}} + \frac{f_{TiN}}{r_{TiN}}\right)} \qquad (20)$$

When $r_{AlN} \approx r_{TiN} = \bar{r}$ and $Z = 2$, it follows that

$$R_G^{'} = \frac{\bar{r}}{3(f_{AlN} + f_{TiN})} \qquad (21)$$

Considering both AlN and TiN together, the calculated particle size $\bar{r}_{cal}$ from equation (21) is given in **Table 9,** which indicates that this equation also cannot provide a satisfactory solution.

Table 9. Evaluations of Particle Size and Austenite Grain Size by Gladman Complex Particles Grain Growth Inhibition Model for Austenitised Ti Steel, only Considering fine TiN particles

T, $^\circ C$	f_{AlN} $\times 10^3$	f_{TiN} $\times 10^3$	$r_{measured}$ nm	$R_{measured}$ μm	$\bar{r}_{cal}$ nm	R_{cal} μm
900	0.813	0.2240		10.7	33.3	
950	0.739	0.2240	21.3	13.5	39.0	7.4
1000	0.647	0.2240		14.2	37.1	
1050	0.537	0.2240		15.7	35.9	
1100	0.402	0.2239	25.1	18.8	25.3	13.4
1150	0.244	0.2237		27.3	38.3	
1200	0.061	0.2235	16.5	34.3	29.3	19.3

Careful metallographical observations on polished specimens by optical microscopy using the highest magnification ($1000\times$) confirmed that in the steel there are a few coarse orange cubic particles and on replicas in the TEM similar particles of about 0.5 - 2.0 μm in edge length gave Ti K_α peaks in EDAX spectra. Compared with the number of TiN fine particles, even if the number of these coarse particles is too small and their size is too large to inhibit of austenite grain growth, the volume fraction of these coarse

TiN, $f_{TiN_{coarse}}$, is significant. According to the solubility data of Ti and N from Gladman [33], the particles precipitated during solidification of the current steel with a composition of 0.012 Ti and 0.018N will take over half of the Ti content to form coarse size of TiN particles. Therefore, the evaluation of the behaviour of austenite grain growth in the Al-V-Ti-N steels obviously requires a consideration of the influence of these coarse particles. Thus, the equation (20) should be rewritten as

$$R_G^{'} = \frac{\left(1-4/3Z\right)}{\left(\frac{f_{AlN}}{r_{AlN}} + \frac{f_{TiN\ fine}}{r_{TiN\ fine}} + \frac{f_{TiN\ coarse}}{r_{TiN\ coarse}}\right)} \qquad (22)$$

$$= \frac{\left(1-4/3Z\right)}{\left\{\frac{1}{\bar{r}}\left(f_{AlN} + F_{TiN\ fine}\right) + \left(\frac{f_{TiN\ coarse}}{r_{TiN\ coarse}}\right)\right\}} \qquad (23)$$

where it is assumed that $r_{AlN} \approx r_{TiN\ fine} = \bar{r}$ and $f_{TiN\ fine} = f_{TiN_{coarse}} = f_{TiN}/2$. When the coarse particle size $r_{TiN_{coarse}}$ is taken as 1 μm, the calculated particle size $\bar{r}_{cal}$ from equation (23) is very close to the measured particle size $r_{measured}$ (see **Table 10**). The influence of the coarse TiN particle size can be seen when the calculation is undertaken at $1200^{\circ}C$ when the ratios in the denominator of equation (22) are respectively f_{AlN}/r_{AlN} = 0.0037, $f_{TiN\ fine}/r_{TiN\ fine}$ = 0.0068 and $f_{TiN\ coarse}/r_{TiN\ coarse}$ = 0.000112. In this example the contribution to $R_G^{'}$ from coarse TiN particles is negligible.

Table 10. Evaluations of Particle Size and Austenite Grain Size by Gladman Complex Particles Grain Growth Inhibition Model for Austenitised Ti Steel, Considering both fine and Coarse TiN particles

T, $^{\circ}C$	f_{AlN} $\times 10^3$	$f_{TiN\ fine}$ = $f_{TiN\ coarse}$ $\times 10^3$	$r_{measured}$ = $r_{AlN} = r_{TiN_{fine}}$ nm	r_{coarse} μm	$R_{measured}$ μm	$\bar{r}_{cal}$ nm	R_{cal} μm
900	0.813	0.112		1.0	10.7	29.8	
950	0.739	0.112	21.3	1.0	13.5	34.6	8.3
1000	0.647	0.112		1.0	14.2	32.5	
1050	0.537	0.112		1.0	15.7	30.7	
1100	0.402	0.112	25.1	1.0	18.8	29.2	16.2
1150	0.244	0.112		1.0	27.3	29.4	
1200	0.061	0.112	16.5	1.0	34.3	18.0	31.4

5. Conclusions

(1) The characteristic features of abnormal austenite grain growth which are related to the presence of pinning particles were observed in the current Al-V-N steels. Estimates of the austenite grain size by six different grain growth inhibition models demonstrated that the best match with the experimental results can be obtained from Gladman and Rios equations and for the present Al-V-N steels, it is, as expected, that AlN and not VC controls the austenite grain size.

(2) The drag force of plate-shaped AlN particles depends on their orientation. The experimental and calculated results indicated that it is probably the average radius of AlN particles which are responsible for controlling austenite grain growth in the low austenising temperature range (900 to 950$^{\circ}C$) and the average length of AlN particles for the high austenising temperature range (1000 to 1200$^{\circ}C$).

(3) Normal austenite grain growth behaviour was followed in the Al-V-Ti-N steel. None of the above six grain growth inhibition models could provide satisfactory predictions when individual particle sizes, of either AlN or TiN, was evaluated independently by each model. A modified Gladman model, which considers the effects of

complex arrays of different types of particles on the stabilized austenite grain size, can be used to predict the austenite grain size and particle size when the combined effect of AlN and TiN is considered. In the general case, both the fine TiN particles precipitated in the solid austenite and the coarse TiN particles precipitated during solidification should be taken into account when the modified Gladman model is employed to predict the austenite grain size.

References

1. M. Hillert, *Acta Metall*., **13**, (1965), 227.

2. K. J. Irvine, F. B. Pickering, and T. Gladman, *J. Iron Steel Inst.*, **205,** (1967), 161.

3. T. Gladman and F. B. Pickering, *J. Iron Steel Inst*., **205**, (1967), 653.

4. T. Gladman, *JOM*. **9**, (1992), 21.

5. F. J. Humphreys and M. Hatherly, *Recrystallization and Related Annealing Phenomena*, Pergamon, Oxford, (1995).

6. T. Gladman, *Proc. Roy. Soc.*, **294A**, (1966), 298.

7. R. Elst, J. Van. Humbeeck, and L. Delaey, *Acta Metall*., **36**, (1988), 1723.

8. I. Andersen, O. Grong and N. Ryum, *Acta Metall*. **43**, (1995), 2689.

9. G. N. Hassold and D. J. Srolovitz, *Scripta Metallurgica*, **32**, (1995), 1541.

10. L. J. Cuddy and J. C. Raley, *Met. Trans. A.*, **14**, (1983), 1989.

11. J. W. Halley, *Trans. AIME*, **167**, (1946), 224.

12. T. Gladman, *Heat Treatment of Metals*, **1**, (1994), 11.

13. H. Adrian and F. B. Pickering, *Mater. Sci. Technol*., **7, (**1991), 176.

14. C. Zener, quoted by C. S. Smith, *Trans. AIME*., **175**, (1948), 47.

15. P. Hellman and M. Hillert, *Scan. J. Met*., **4**, (1975), 211.

16. M. Hillert, *Acta Metall*., **36**, (1988), 3177.

17. P. R. Rios, *Acta Metall*., **35**, (1987), 2805.

18. D. J. Senogles, Ph.D Thesis, University of Leeds, (1994).

19. B. Aronsson, *Climax Molybdenum Special Publication*, (1973), 77.

20. P. Konig, W. Scholz, and H. Ulmer, *Archs Eisenhutt*., **32**, (1961), 541.

21. N. Gao, PhD Thesis, University of Strathclyde, (1997).

22. C. J. Tweed, N. Hansen, and B. Ralph, *Met. Trans. A.*, **14A**, (1983), 2235.

23. J. Strid and K. E. Easterling, *Acta Metall*., **33**, (1985), 2057.

24. N. Ryum, O. Hunderi and E. Nes, *Scripta Metallurgica et Materialia*. **17**, (1983), 1281.

25. W. B. Li and K. E. Easterling, *Acta Metall*., **38**, (1990), 1045.

26. C. H. Worner and P. M. Hazzledine, *JOM*. **9**, (1992), 16.

27. S. P. Ringer, W. B. Li and K. E. Easterling, *Acta Metall*., **37**, (1989), 831.

28. W. Roberts, in Proc. Conf. *'HSLA Steels, Technology and Applications'* ed. M. Korchynsky, Philadelphia, ASM, (1984), 33.

29. K. A. El-Fawakhry, M. F. Mekkawy and M. L. Mishreky, *ISIJ International*, **31**, (1991), 1020.

30. N. Gao and T. N. Baker, *ISIJ International*, **37**, (1997), 602.

31. T. Gladman and Q. Li, in *'35th MWSP Conf. Proc*.', ISS-AIME, **31**, (1994), 453.

32. T. Gladman and D. J. Senogles, in Proc. Conf. *'Titanium Technology in Microalloyed Steels'*, ed. T. N. Baker, The Institute of Materials, (1997), 83.

33. T. Gladman, *The Physical Metallurgy of Microalloyed Steels*, Inst. Mat., London, 1997.